

Determination of nonlinear refractive index in a Ta₂O₅ rib waveguide using self-phase modulation

Chao-Yi Tai and James S. Wilkinson

Optoelectronics Research Centre, University of Southampton, Highfield, Southampton, SO17 1BJ, United Kingdom
cvt@orc.soton.ac.uk

Nicolas M. B. Perney and M. Caterina Netti

Mesophotonics Limited, Chilworth Business Incubator, 2 Venture Road, Chilworth Science Park, Southampton, SO16 7NP, United Kingdom

F. Cattaneo, Chris E. Finlayson, and Jeremy J. Baumberg

School of Physics and Astronomy, University of Southampton, Highfield, Southampton, SO17 1BJ, United Kingdom

Abstract: Self-phase modulation has been observed for ultrashort pulses of wavelength 800nm propagating through a 1 cm-long Ta₂O₅ rib waveguide. The associated nonlinear refractive index n_2 was estimated to be $7.23 \times 10^{-19} \text{ m}^2/\text{W}$, which is higher than silica glass by more than one order of magnitude. Femtosecond time of flight measurements based on a Kerr shutter configuration show that the group velocity dispersion is small at a wavelength of 800 nm, confirming that dispersion may be neglected in the estimation of n_2 so that a simplified theory can be used with good accuracy.

©2004 Optical Society of America

OCIS codes: (190.0190) Nonlinear Optics; (160.4670) Optical materials.

References and links

1. B. P. Nelson, K. J. Blow, P. D. Constantine, N. J. Doran, J. K. Lucek, I. W. Marshall, and K. Smith, "All-optical Gbit/s switching using nonlinear optical loop mirror," *Electron. Lett.* **27**, 704-705 (1991).
2. A. Samoc, M. Samoc, M. Woodruff, and B. Luther-Davies, "Tuning the properties of poly(p-phenylenevinylene) for use in all-optical switching," *Opt. Lett.* **20**, 1241-1243 (1995).
3. M. Asobe, I. Yokohama, T. Kaino, S. Tomaru, and T. Kurihara, "Nonlinear absorption and refraction in an organic-dye functionalized main-chain polymer wave-guide in the 1.5 μm wavelength region," *Appl. Phys. Lett.* **67**, 891-893 (1995).
4. T. Gabler, R. Waldhäusl, A. Bräuer, F. Michelotti, H. -H. Hörhold, and U. Bartuch, "Spectral broadening measurements in poly(phenylene vinylene) polymer channel waveguides," *Appl. Phys. Lett.* **70**, 928-930 (1997).
5. M. Asobe, K. Suzuki, T. Kanamori, and K. Kubodera, "Nonlinear refractive-index measurement in chalcogenide-glass fibers by self-phase modulation," *Appl. Phys. Lett.* **60**, 1153-1154 (1992).
6. T. Kobayashi, *Nonlinear Optics of Organics and Semiconductors* (Springer, Berlin, 1989).
7. P. C. Joshi and M. W. Cole, "Influence of postdeposition annealing on the enhanced structural and electrical properties of amorphous and crystalline Ta₂O₅ thin films for dynamic random access memory applications," *J. Appl. Phys.* **86**, 871-880 (1999).
8. E. Franke, C. L. Trimble, M. J. DeVries, J. A. Woollam, M. Schubert, and F. Frost, "Dielectric function of amorphous tantalum oxide from the far infrared to the deep ultraviolet spectral region measured by spectroscopic ellipsometry," *J. Appl. Phys.* **88**, 5166-5174 (2000).
9. J. Jasapara, A. V. V. Nampoothiri, and W. Rudolph, "Femtosecond laser pulse induced breakdown in dielectric thin films," *Phys. Rev. B* **63**, 045117 (2001).
10. G. P. Agrawal, *Nonlinear Fiber Optics*, (Academic, San Diego, 1989).
11. P. N. Kean, K. Smith, and W. Sibbett, "Spectral and temporal investigation of self-phase modulation and stimulated Raman scattering in a single-mode optical fibre," *IEE Proc. J. Optoelectron.* **134**, 163-170 (1987).
12. B. M. Foley, P. Melman, and K. T. Vo, "Novel loss measurement technique for optical wave-guides by imaging of scattered-light," *Electron. Lett.* **28**, 584-585 (1992).

13. J. Requejo-Isidro, A. K. Mairaj, V. Pruneri, D. W. Hewak, M. C. Netti, and J. J. Baumberg, "Self-refractive non-linearities in chalcogenide based glasses," *J. Non-Cryst. Solids* **317**, 241-246 (2003).
 14. M. Asobe, T. Kanamori, and K. Kubodera, "Applications of highly nonlinear chalcogenide glass fibers in ultrafast all-optical switches," *IEEE J Quantum Electron.* **29**, 2325-2333 (1993).
 15. M. C. Netti, C. E. Finlayson, J. J. Baumberg, M. D. B. Charlton, M. E. Zoorob, J. S. Wilkinson and G. J. Parker, "Separation of photonic crystal waveguides modes using femtosecond time-of-flight," *Appl. Phys. Lett.* **81**, 3927-3929 (2002).
 16. J. Takeda, K. Nakajima, and S. Kurita, "Time-resolved luminescence spectroscopy by the optical Kerr-gate method applicable to ultrafast relaxation processes," *Phys. Rev. B* **62**, 10083-10087 (2000).
-

1. Introduction

Reliable, efficient generation of high peak power, ultrashort laser pulses has allowed the exploitation of many new material phenomena and, in particular, is stimulating intensive research into nonlinear optical effects. Ultrafast all-optical switching devices will play an increasingly important role in modern optical communication systems where signals are transmitted at high speed and high-bit-rate. Nonlinear refraction which exploits third-order electronic polarization has a subpicosecond response time and is thus suitable for high speed switching. Silica optical fibers have been widely used for all-optical switching due to their low loss and long interaction length. However, the small nonlinear refractive index of silica, n_2 ($\sim 2.2 \times 10^{-20} \text{ m}^2/\text{W}$) [1], requires high switching power and a very long length of fiber to achieve useful optical switching. Although many materials with higher nonlinear refractive index have been reported [2-6], there is a need to explore alternatives, particularly those compatible with planar processing technology, due to the rapid growth of planar devices such as wavelength division multiplexers and add-drop filters in advanced networks. To achieve compact low-power high-speed switching devices, a large nonlinear refractive index (n_2) is required. In addition, materials with minimal loss and absorption at the operating wavelength, a fast response, low toxicity with highly thermal and mechanical stability are preferred. Ta_2O_5 has been widely used as gate material for microelectronic devices, due to its high dielectric constant [7]. The correspondingly high refractive index at optical frequencies offers great potential for making compact waveguide and photonic crystal devices with small effective area, enabling the exploitation of nonlinear effects at low power. The wide material bandgap and transparency over a broad spectral range [8] also avoids severe two-photon absorption (TPA), which limits the attainable nonlinear phase shift in most semiconductors. Moreover, its high laser damage threshold [9] further broadens its application particularly to devices employing ultrashort high-peak power optical pulses. Although Ta_2O_5 is widely used for multilayer dielectric mirrors, there are no reports to our knowledge on its optical nonlinearity to date.

In this letter, we present an experimental measurement of the nonlinear refractive index in a Ta_2O_5 rib waveguide, based on self-phase modulation (SPM) induced spectral broadening. The impact of group velocity dispersion (GVD) is also discussed in the femtosecond time of flight measurements.

2. Waveguide fabrication and experimental methods

The waveguide under investigation was fabricated by sputtering a 1 μm thick Ta_2O_5 film onto a Si wafer, on which a 2 μm thick SiO_2 buffer layer had been grown. Photolithography and argon ion beam milling were then used to create rib waveguides in the Ta_2O_5 with a width of 3 μm and a depth of 1 μm . The wafer was then cleaved into chips of 10mm length to allow end-fire coupling of light.

A diode-pumped frequency-doubled Nd:YVO₄ laser, producing single frequency output at $\lambda=532 \text{ nm}$, was used to pump a Ti-Sapphire laser which generated sub-150 femtosecond, linearly polarized, modelocked pulses at $\lambda=800 \text{ nm}$ with a repetition rate of 80 MHz. These pulses seeded a regenerative amplifier system (RegA) working at a 250 kHz repetition rate. Nearly transform-limited pulses with duration at full width half maximum of $\Delta t_{\text{FWHM}}=160 \text{ fs}$ were obtained and end-fire launched into the rib waveguide using a microscope objective lens.

The light emerging from the waveguide was collected and directed into a high resolution spectrum analyzer without passing through any other optical components. The incident power was controlled by using calibrated neutral density filters and the modal intensity profile was monitored using a CCD camera to confirm single mode operation of the rib waveguide and to determine the modal spotsize. Due to the linear polarization of the Ti-Sapphire source, all our subsequent measurements reported here relate to the TE mode of propagation through the waveguide.

3. SPM induced spectra

Figure 1(a) shows the spectrum of the incident pulses from the regenerative amplifier, while Fig. 1(b-d) shows the observed spectral evolution of the transform-limited Gaussian pulse emerging from a 1-cm-long rib waveguide at various peak-coupled powers, taking account of a measured coupling loss of 18 dB. As the peak power in the waveguide was increased, the output spectrum broadened significantly, accompanied by the development of oscillatory structures with intense outermost peaks. This multipeak structure, arising from the interference of the chirped frequency components induced by SPM, is the signature of SPM spectra [10] and is clearly in evidence in Fig. 1.

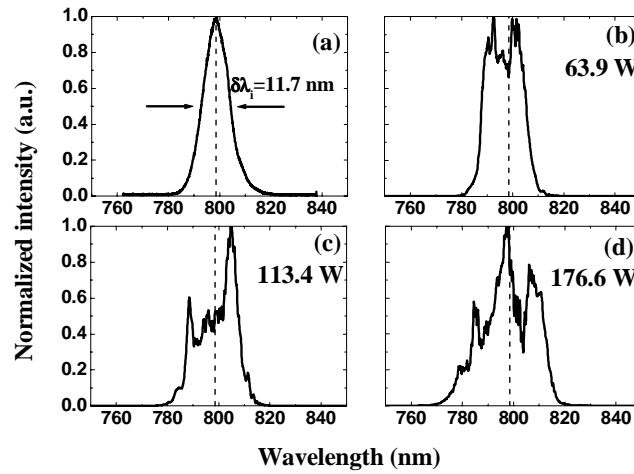


Fig. 1. (a) Spectrum of the incident radiation; (b), (c) & (d) Observed self-phase modulation output spectra at peak coupled powers of 63.9 W, 113.4 W, and 176.6 W, respectively.

To calculate the nonlinear refractive index, n_2 , a simplified theory which ignores the influence of GVD was employed as the lowest-order approach [10]. The SPM-induced frequency shift is a consequence of a temporally varying phase and can be expressed in terms of the intensity-dependent refractive index n_2 as

$$\delta\omega = -\frac{\partial\phi_{NL}}{\partial t} = -\frac{2\pi}{\lambda} n_2 L_{eff} \frac{dI(t)}{dt} \quad (1)$$

where $I(t)$ is the temporal intensity profile of the incident pulse and L_{eff} is the effective length defined by

$$L_{eff} = \frac{1 - \exp(-\alpha L)}{\alpha} \quad (2)$$

in which L is the physical sample length and α is the attenuation constant. For an unchirped Gaussian input pulse, the full width half maximum (FWHM) spectral bandwidth, $\delta\lambda$, of the SPM pulse can be found from Eq. (1) to be [11]:

$$\delta\lambda = \delta\lambda_i + 4\sqrt{\frac{2 \ln 2}{e}} \frac{\lambda n_2 L_{\text{eff}}}{c A_{\text{eff}}} \frac{P}{t_p} \quad (3)$$

where $\delta\lambda_i$ and t_p represent the bandwidth and pulsewidth of the input laser pulse, respectively. P is the peak input power and A_{eff} is the effective core area defined by:

$$A_{\text{eff}} = \frac{\left[\iint F(x, y)^2 dx dy \right]^2}{\iint F(x, y)^4 dx dy} \quad (4)$$

where $F(x,y)$ is the modal intensity distribution. Figure 2 shows the SPM-induced spectral bandwidth, $\delta\lambda$, against the peak coupled power with a linear least-squares fit to the data points. Extrapolating the line to $P=0$, representing the bandwidth of the input pulse, yields an intercept value of 12 ± 0.4 nm, which is in good agreement with the recorded input spectrum ($\delta\lambda_i = 11.7 \pm 0.39$ nm), as shown in Fig. 1(a). The nonlinear refractive index, n_2 , was estimated from Eq. (3) using the fitted slope (0.083 nm/W), and the following values for the other parameters: $\alpha = 0.345 \text{ cm}^{-1}$ measured by imaging of scattered light [12], $L = 1$ cm, $A_{\text{eff}} = (3.5 \pm 0.18) \mu\text{m}^2$ estimated from the recorded modal intensity profile [10], $\lambda = 800$ nm and $t_p = 160$ fs. In this way, the intensity-dependent refractive index n_2 was found to be $(7.23 \pm 0.36) \times 10^{-19} \text{ m}^2/\text{W}$, which is higher than silica glass ($n_2 \sim 2.2 \times 10^{-20} \text{ m}^2/\text{W}$) by more than one order of magnitude. Although the value is smaller than chalcogenide and sulfur based glasses [13], Ta_2O_5 has the advantages of wide transparency in the telecommunication window and low toxicity in fabrication process. We note that this simple analysis does not produce a realistic calculation of uncertainty limits, such as that of integration of the nonlinear Schrödinger equation for SPM might facilitate. The error bar in the estimation of n_2 here originated merely from an estimation of uncertainty in the effective area. However, we do not consider that such considerations will have any significant bearing upon the order of magnitude effects we calculate.

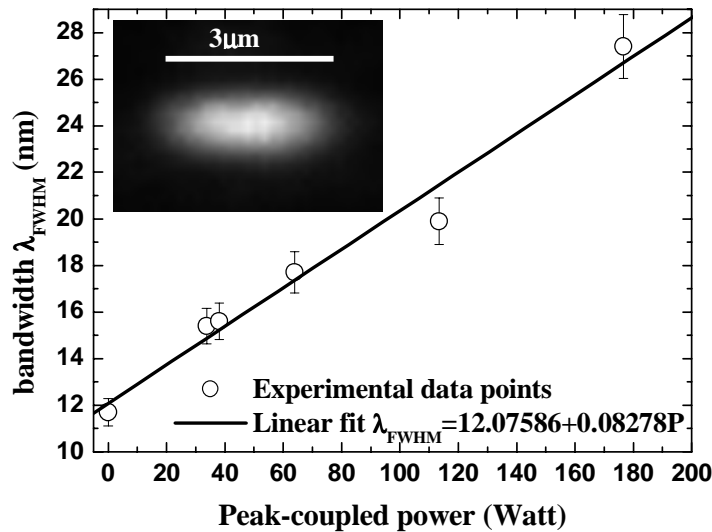


Fig. 2. SPM spectral bandwidth against peak-coupled power; the inset shows the modal intensity profile from the rib waveguide.

4. Time of flight measurement

This value of n_2 was obtained under the assumption that the group velocity dispersion (GVD) has a negligible impact on the pulse shape. To ascertain the validity of this assumption, femtosecond time of flight measurement, based on a Kerr shutter configuration [14,15] as shown in Fig. 3, was used to investigate the GVD effect. The optical Kerr shutter was composed of a 1 mm thick SFL6 glass plate between two crossed polarizers. SFL6 glass has a high third-order nonlinear susceptibility which responds to the pump pulse almost instantaneously [16]. When a pump pulse (150 mW, $\lambda=800$ nm, 160fs) is incident on the glass plate, a transient birefringence is induced, allowing the ultrabroadband white light continuum probe pulse (from 450 nm to 1100 nm) to pass through. In order to exclude the intense component at $\lambda=800$ nm, and prevent damage to the detector, a hot mirror was used to cut out wavelengths longer than 710nm. The time delay of the pump pulse was scanned, and the spectrum of the resultant gated signal at each time delay was analyzed on a spectrum analyzer and recorded. The time of flight for the fundamental waveguide mode was obtained by subtracting the delay when sample is absent from the measured delay time, to eliminate the system dispersion.

Figure 4 (black line) shows the time of flight spectrum of the fundamental TE mode propagates through the rib waveguide. The curve was extrapolated to $\lambda=850$ nm using a polynomial fit. The dispersion parameter (D), obtained from the differentiation of the time of flight spectrum, was also plotted (blue line). From this figure, it should be noted that the dispersion is very small at $\lambda=800$ nm, where the SPM measurement was performed. The GVD (β_2) at $\lambda=800$ nm was calculated from $\beta_2=(-D\lambda^2/2\pi c)$ and yield a value of 246 fs²/cm. This value results in a dispersion length $L_D=t_p^2/\beta_2=104$ cm, which is much larger than the sample length ($L=1$ cm) indicating a negligible impact at $\lambda=800$ nm. The hatched region shown in Fig. 4 is where the dispersion length $L_D > 10$ cm. It clearly shows that we are well within the region, where GVD has a negligible impact, with wide tolerance. This result confirms the validity of the simplified theory used for the estimation of the nonlinear refractive index.

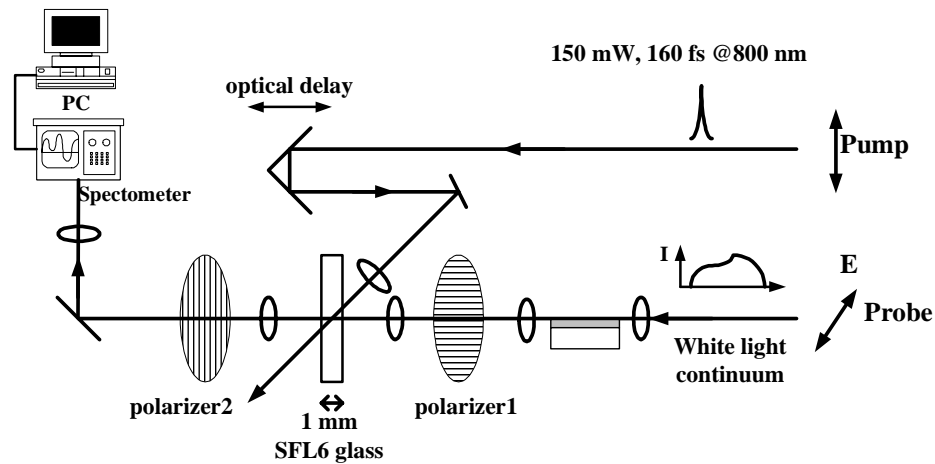


Fig. 3. Experimental configuration for femtosecond time-of-flight measurements.

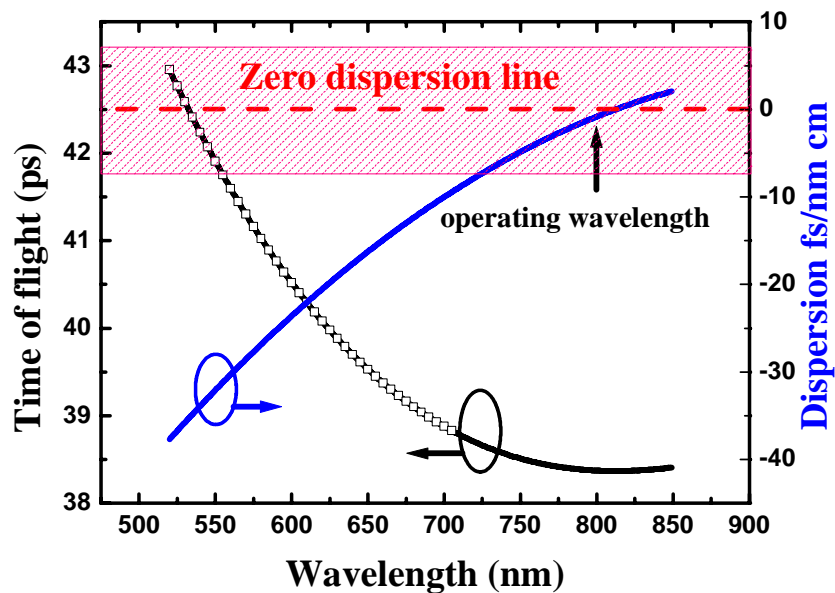


Fig. 4. Time-of-flight spectra (black line) and dispersion (blue line) for the fundamental TE mode.

5. Conclusion

In conclusion, we have demonstrated the measurement of the nonlinear refractive index of a Ta_2O_5 rib waveguide by directly monitoring the output spectra broadened by self phase modulation. Using a simplified theory which assumes that the group velocity dispersion has a negligible effect, the nonlinear refractive index was determined to be $n_2=(7.23\pm 0.36)\times 10^{-19} \text{ m}^2/\text{W}$, which is larger than the value of silica glass ($n_2\sim 2.2\times 10^{-20} \text{ m}^2/\text{W}$) by more than one

order of magnitude. Femtosecond time of flight measurements based on a Kerr shutter configuration show that the group velocity dispersion has a negligible impact upon the spectral broadening within a 1-cm-long sample at $\lambda=800\text{nm}$, which confirms the validity and of the approximation used in the estimation. This large value of n_2 in Ta_2O_5 , in conjunction with its high index and excellent compatibility with present silicon/silica processing technologies, makes it a promising candidate for compact, low-power, high-speed, and all-optical planar switching devices.